Measurement of Transverse Single-Spin Asymmetries for Midrapidity Production of Neutral Pions and Charged Hadrons in Polarized $p + p$ Collisions at $\sqrt{s} = 200$ GeV

S. S. Adler,[5] S. Afanasiev,[17] C. Aidala,[5] N. N. Ajitanand,[43] Y. Akiba,[20,38] J. Alexander,[43] R. Amirikas,[12] L. Aphecetche,[45] S. H. Aronson,[5] R. Averbeck,[44] T. C. Awes,[35] R. Azmoun,[44] V. Babintsev,[15] A. Baldisseri,[10] K. N. Barish,[6] P. D. Barnes,[27] B. Bassalleck,[33] S. Bathe,[30] S. Batsouli,[9] V. Baublis,[37] F. Bauer,[6] A. Bazilevsky,[39,15] S. Belikov,[16,15] Y. Berdnikov,[40] S. Bhagavatula,[16] J. G. Boissevain,[27] H. Borel,[10] S. Borenstein,[25] M. L. Brooks,[27] D. S. Brown,[34] N. Bruner,[33] D. Bucher,[30] H. Buesching,[30] V. Bumazhnov,[15] G. Bunce,[5,39] J. M. Burward-Hoy,[26,44] S. Butsyk,[44] X. Camard,[45] J.-S. Chai,[18] P. Chand,[4] W. C. Chang,[2] S. Chernichenko,[15] C. Y. Chi,[9] J. Chiba,[20] M. Chiu,[9] I. J. Choi,[52] J. Choi,[19] R. K. Choudhury,[4] T. Chujo,[5] V. Cianciolo,[35] Y. Cobigo,[10] B. A. Cole,[9] P. Constantin,[16] D. d'Enterria,[45] G. David,[5] H. Delagrange,[45] A. Denisov,[15] A. Deshpande,[39] E. J. Desmond,[5] A. Devismes,[44] O. Dietzsch,[41] O. Drapier,[25] A. Drees,[44] K. A. Drees,[5] R. du Rietz,[29] A. Durum,[15] D. Dutta,[4] Y. V. Efremenko,[35] K. El Chenawi,[49] A. Enokizono,[14] H. En'yo,[38,39] S. Esumi,[48] L. Ewell,[5] D. E. Fields,[33,39] F. Fleuret,[25] S. L. Fokin,[23] B. D. Fox,[39] Z. Fraenkel,[51] J. E. Frantz,[9] A. Franz,[5] A. D. Frawley,[12] S.-Y. Fung,[6] S. Garpman,[29,*] T. K. Ghosh,[49] A. Glenn,[46] G. Gogiberidze,[46] M. Gonin,[25] J. Gosset,[10] Y. Goto,[39] R. Granier de Cassagnac,[25] N. Grau,[16] S. V. Greene,[49] M. Grosse Perdekamp,[39] W. Guryn,[5] H.-Å. Gustafsson,[29] T. Hachiya,[14] J. S. Haggerty,[5] H. Hamagaki,[8] A. G. Hansen,[27] E. P. Hartouni,[26] M. Harvey,[5] R. Hayano,[8] N. Hayashi,[38] X. He,[13] M. Heffner,[26] T. K. Hemmick,[44] J. M. Heuser,[44] M. Hibino,[50] J. C. Hill,[16] W. Holzmann,[43] K. Homma,[14] B. Hong,[22] A. Hoover,[34] T. Ichihara,[38,39] V. V. Ikonnikov,[23] K. Imai,[24,38] D. Isenhower,[1] M. Ishihara,[38] M. Issah,[43] A. Isupov,[17] B. V. Jacak,[44] W. Y. Jang,[22] Y. Jeong,[19] J. Jia,[44] O. Jinnouchi,[38] B. M. Johnson,[5] S. C. Johnson,[26] K. S. Joo,[31] D. Jouan,[36] S. Kametani,[8,50] N. Kamihara,[47,38] J. H. Kang,[52] S. S. Kapoor,[4] K. Katou,[50] S. Kelly,[9] B. Khachaturov,[51] A. Khanzadeev,[37] J. Kikuchi,[50] D. H. Kim,[31] D. J. Kim,[52] D. W. Kim,[19] E. Kim,[42] G.-B. Kim,[25] H. J. Kim,[52] E. Kistenev,[5] A. Kiyomichi,[48] K. Kiyoyama,[32] C. Klein-Boesing,[30] H. Kobayashi,[38,39] L. Kochenda,[37] V. Kochetkov,[15] D. Koehler,[33] T. Kohama,[14] M. Kopytine,[44] D. Kotchetkov,[6] A. Kozlov,[51] P. J. Kroon,[5] C. H. Kuberg,[1,27,*] K. Kurita,[39] Y. Kuroki,[48] M. J. Kweon,[22] Y. Kwon,[52] G. S. Kyle,[34] R. Lacey,[43] V. Ladygin,[17] J. G. Lajoie,[16] A. Lebedev,[16,23] S. Leckey,[44] D. M. Lee,[27] S. Lee,[19] M. J. Leitch,[27] X. H. Li,[6] H. Lim,[42] A. Litvinenko,[17] M. X. Liu,[27] Y. Liu,[36] C. F. Maguire,[49] Y. I. Makdisi,[5] A. Malakhov,[17] V. I. Manko,[23] Y. Mao,[7,38] G. Martinez,[45] M. D. Marx,[44] H. Masui,[48] F. Matathias,[44] T. Matsumoto,[8,50] P. L. McGaughey,[27] E. Melnikov,[15] F. Messer,[44] Y. Miake,[48] J. Milan,[43] T. E. Miller,[49] A. Milov,[44,51] S. Mioduszewski,[5] R. E. Mischke,[27] G. C. Mishra,[13] J. T. Mitchell,[5] A. K. Mohanty,[4] D. P. Morrison,[5] J. M. Moss,[27] F. Mühlbacher,[44] D. Mukhopadhyay,[51] M. Muniruzzaman,[6] J. Murata,[38,39] S. Nagamiya,[20] J. L. Nagle,[9] T. Nakamura,[14] B. K. Nandi,[6] M. Nara,[48] J. Newby,[46] P. Nilsson,[29] A. S. Nyanin,[23] J. Nystrand,[29] E. O'Brien,[5] C. A. Ogilvie,[16] H. Ohnishi,[5,38] I. D. Ojha,[49,3] K. Okada,[38] M. Ono,[48] V. Onuchin,[15] A. Oskarsson,[29] I. Otterlund,[29] K. Oyama,[8] K. Ozawa,[8] D. Pal,[51] A. P. T. Palounek,[27] V. Pantuev,[44] V. Papavassiliou,[34] J. Park,[42] A. Parmar,[33] S. F. Pate,[34] T. Peitzmann,[30] J.-C. Peng,[27] V. Peresedov,[17] C. Pinkenburg,[5] R. P. Pisani,[5] F. Plasil,[35] M. L. Purschke,[5] A. K. Purwar,[44] J. Rak,[16] I. Ravinovich,[51] K. F. Read,[35,46] M. Reuter,[44] K. Reygers,[30] V. Riabov,[37,40] Y. Riabov,[37] G. Roche,[28] A. Romana,[25] M. Rosati,[16] P. Rosnet,[28] S. S. Ryu,[52] M. E. Sadler,[1] N. Saito,[38,39] T. Sakaguchi,[8,50] M. Sakai,[32] S. Sakai,[48] V. Samsonov,[37] L. Sanfratello,[33] R. Santo,[30] H. D. Sato,[24,38] S. Sato,[5,48] S. Sawada,[20] S. Schutz,[45] V. Semenov,[15] R. Seto,[6] M. R. Shaw,[1,27] T. K. Shea,[5] T.-A. Shibata,[47,38] K. Shigaki,[14,20] T. Shiina,[27] C. L. Silva,[41] D. Silvermyr,[27,29] K. S. Sim,[22] C. P. Singh,[3] V. Singh,[3] M. Sivertz,[5] A. Soldatov,[15] R. A. Soltz,[26] W. E. Sondheim,[27] S. P. Sorensen,[46] I. V. Sourikova,[5] F. Staley,[10] P. W. Stankus,[35] E. Stenlund,[29] M. Stepanov,[34] A. Ster,[21] S. P. Stoll,[5] T. Sugitate,[14] J. P. Sullivan,[27] E. M. Takagui,[41] A. Taketani,[38,39] M. Tamai,[50] K. H. Tanaka,[20] Y. Tanaka,[32] K. Tanida,[38] M. J. Tannenbaum,[5] P. Tarján,[11] J. D. Tepe,[1,27] T. L. Thomas,[33] J. Tojo,[24,38] H. Torii,[24,38] R. S. Towell,[1] I. Tserruya,[51] H. Tsuruoka,[48] S. K. Tuli,[3] H. Tydesjö,[29] N. Tyurin,[15] H. W. van Hecke,[27] J. Velkovska,[5,44] M. Velkovsky,[44] V. Veszprémi,[11] L. Villatte,[46] A. A. Vinogradov,[23] M. A. Volkov,[23] E. Vznuzdaev,[37] X. R. Wang,[13] Y. Watanabe,[38,39] S. N. White,[5] F. K. Wohn,[16] C. L. Woody,[5] W. Xie,[6] Y. Yang,[7] A. Yanovich,[15] S. Yokkaichi,[38,39] G. R. Young,[35] I. E. Yushmanov,[23] W. A. Zajc,[9,†] C. Zhang,[9] S. Zhou,[7] S. J. Zhou,[51] and L. Zolin[17]

(PHENIX Collaboration)

[1]*Abilene Christian University, Abilene, Texas 79699, USA*
[2]*Institute of Physics, Academia Sinica, Taipei 11529, Taiwan*
[3]*Department of Physics, Banaras Hindu University, Varanasi 221005, India*

[4]Bhabha Atomic Research Centre, Bombay 400 085, India

[5]Brookhaven National Laboratory, Upton, New York 11973-5000, USA

[6]University of California—Riverside, Riverside, California 92521, USA

[7]China Institute of Atomic Energy (CIAE), Beijing, People's Republic of China

[8]Center for Nuclear Study, Graduate School of Science, University of Tokyo, 7-3-1 Hongo, Bunkyo, Tokyo 113-0033, Japan

[9]Columbia University, New York, New York 10027, USA,
and Nevis Laboratories, Irvington, New York 10533, USA

[10]Dapnia, CEA Saclay, F-91191 Gif-sur-Yvette, France

[11]Debrecen University, H-4010 Debrecen, Egyetem tér 1, Hungary

[12]Florida State University, Tallahassee, Florida 32306, USA

[13]Georgia State University, Atlanta, Georgia 30303, USA

[14]Hiroshima University, Kagamiyama, Higashi-Hiroshima 739-8526, Japan

[15]IHEP Protvino, State Research Center of Russian Federation, Institute for High Energy Physics, Protvino 142281, Russia

[16]Iowa State University, Ames, Iowa 50011, USA

[17]Joint Institute for Nuclear Research, 141980 Dubna, Moscow Region, Russia

[18]KAERI, Cyclotron Application Laboratory, Seoul, South Korea

[19]Kangnung National University, Kangnung 210-702, South Korea

[20]KEK, High Energy Accelerator Research Organization, Tsukuba, Ibaraki 305-0801, Japan

[21]KFKI Research Institute for Particle and Nuclear Physics of the Hungarian Academy of Sciences (MTA KFKI RMKI),
H-1525 Budapest 114, P.O. Box 49, Budapest, Hungary

[22]Korea University, Seoul 136-701, Korea

[23]Russian Research Center "Kurchatov Institute," Moscow, Russia

[24]Kyoto University, Kyoto 606-8502, Japan

[25]Laboratoire Leprince-Ringuet, Ecole Polytechnique, CNRS-IN2P3, Route de Saclay, F-91128 Palaiseau, France

[26]Lawrence Livermore National Laboratory, Livermore, California 94550, USA

[27]Los Alamos National Laboratory, Los Alamos, New Mexico 87545, USA

[28]LPC, Université Blaise Pascal, CNRS-IN2P3, Clermont-Fd, 63177 Aubiere Cedex, France

[29]Department of Physics, Lund University, Box 118, SE-221 00 Lund, Sweden

[30]Institut für Kernphysik, University of Muenster, D-48149 Muenster, Germany

[31]Myongji University, Yongin, Kyonggido 449-728, Korea

[32]Nagasaki Institute of Applied Science, Nagasaki-shi, Nagasaki 851-0193, Japan

[33]University of New Mexico, Albuquerque, New Mexico 87131, USA

[34]New Mexico State University, Las Cruces, New Mexico 88003, USA

[35]Oak Ridge National Laboratory, Oak Ridge, Tennessee 37831, USA

[36]IPN-Orsay, Universite Paris Sud, CNRS-IN2P3, BP 1, F-91406 Orsay, France

[37]PNPI, Petersburg Nuclear Physics Institute, Gatchina, Russia

[38]RIKEN, The Institute of Physical and Chemical Research, Wako, Saitama 351-0198, Japan

[39]RIKEN BNL Research Center, Brookhaven National Laboratory, Upton, New York 11973-5000, USA

[40]Saint Petersburg State Polytechnic University, St. Petersburg, Russia

[41]Universidade de São Paulo, Instituto de Física, Caixa Postal 66318, São Paulo CEP05315-970, Brazil

[42]System Electronics Laboratory, Seoul National University, Seoul, South Korea

[43]Chemistry Department, Stony Brook University, SUNY, Stony Brook, New York 11794-3400, USA

[44]Department of Physics and Astronomy, Stony Brook University, SUNY, Stony Brook, New York 11794, USA

[45]SUBATECH (Ecole des Mines de Nantes, CNRS-IN2P3, Université de Nantes) BP 20722-44307, Nantes, France

[46]University of Tennessee, Knoxville, Tennessee 37996, USA

[47]Department of Physics, Tokyo Institute of Technology, Tokyo 152-8551, Japan

[48]Institute of Physics, University of Tsukuba, Tsukuba, Ibaraki 305, Japan

[49]Vanderbilt University, Nashville, Tennessee 37235, USA

[50]Advanced Research Institute for Science and Engineering, Waseda University,
17 Kikui-cho, Shinjuku-ku, Tokyo 162-0044, Japan

[51]Weizmann Institute, Rehovot 76100, Israel

[52]Yonsei University, IPAP, Seoul 120-749, Korea

Transverse single-spin asymmetries to probe the transverse-spin structure of the proton have been measured for neutral pions and nonidentified charged hadrons from polarized proton-proton collisions at midrapidity and $\sqrt{s} = 200$ GeV. The data cover a transverse momentum (p_T) range 1.0–5.0 GeV/c for neutral pions and 0.5–5.0 GeV/c for charged hadrons, at a Feynman-x value of approximately zero. The asymmetries seen in this previously unexplored kinematic region are consistent with zero within errors of a few percent. In addition, the inclusive charged hadron cross section at midrapidity from $0.5 < p_T < 7.0$ GeV/c is presented and compared to next-to-leading order perturbative QCD (pQCD) calculations.

Successful description of the unpolarized cross section above ~ 2 GeV/c suggests that pQCD is applicable in the interpretation of the asymmetry results in the relevant kinematic range.

The spin structure of the proton persists as an intricate problem in quantum chromodynamics (QCD). In particular, its transverse-spin structure remains poorly understood. The measurement of transverse single-spin asymmetries (SSAs) in proton-proton collisions and lepton-nucleon deep-inelastic scattering (DIS) probes the quark and gluon structure of transversely polarized nucleons. Interest in these measurements is heightened by the large transverse SSAs observed in spin-dependent proton-proton scattering experiments spanning a wide range of energies. At $\sqrt{s} = 5$–10 GeV, asymmetries approaching 30% were seen in forward inclusive pion production [1,2]. At midrapidity, asymmetries were also observed in inclusive π^0 and π^+ but not π^- production [3–5]. At higher center-of-mass energies of 20 and 200 GeV, π^+, π^-, and π^0 asymmetries were found to persist at large Feynman-x (x_F) [6–8] while the asymmetry in π^0 production at midrapidity was found to be consistent with zero at $\sqrt{s} = 20$ GeV [9]. Nonzero transverse asymmetries have also been observed in semi-inclusive DIS experiments [10–12].

Three different mechanisms have been studied as the possible origin of transverse SSAs in hadron collisions at high energies: (1) Transversity distributions, the quark spin distributions in a transversely polarized proton, can give rise to SSAs in combination with spin-dependent fragmentation functions (FFs), e.g., the Collins function [13]. Spin-dependent FFs serve as analyzers for the transverse spin of the struck quark. (2) Quark and gluon distributions that are asymmetric in the transverse intrinsic parton momentum, k_T, first suggested by Sivers [14], can lead to SSAs. (3) Alternatively, interference between quark and gluon fields in the initial or final state can also generate SSAs [15,16]. Sivers parton distributions can exist for both quarks and gluons, and a possible connection to orbital angular momentum of partons in the nucleon has been suggested [14,17].

It is expected that SSAs measured at the Relativistic Heavy Ion Collider (RHIC) result from a combination of these three effects (see [8], and references therein). Model calculations leading to predictions for the Sivers and transversity distributions have been performed to describe existing data at forward rapidities. Precision measurements of SSAs in different regions of x_F and transverse momentum (p_T) and their QCD analysis may serve to quantify contributions from the competing mechanisms. In this Letter, we present first measurements of transverse single-spin asymmetries at midrapidity and collider energies.

These data were collected during the 2001–2002 polarized proton run at RHIC, in which approximately 0.15 pb^{-1} of integrated luminosity were collected using the PHENIX detector. Two beams of 55 bunches of polarized protons, with approximately 5×10^{10} protons per bunch, were injected into RHIC and accelerated to 100 GeV each.

Measurements of the unpolarized production of charged hadrons and of the spin-dependent production of neutral pions and charged hadrons were made in the central arms of the PHENIX detector. These cover a pseudorapidity range $|\eta| < 0.35$ and two azimuthal angle intervals of 90°, offset 33.75° from vertical [18].

A minimum-bias (MB) collision trigger and the vertex position in the beam direction are provided by two beam-beam counters (BBCs) [19]. The BBCs, which cover 2π in azimuth and $3.0 < |\eta| < 3.9$, are sensitive to charged particles and select approximately half of the total inelastic proton-proton cross section. A ± 30 cm event vertex cut was applied for all analyses, corresponding to the central arm acceptance. The approximate vertex resolution was 2 cm in the beam direction.

Charged-particle tracks from MB events were reconstructed using a drift chamber and pad chambers [20] as well as the collision vertex, which is the assumed point of origin because the tracking chambers are placed outside the magnetic field. Thus charged particles that do not originate at the vertex have incorrectly reconstructed momentum, leading to low-momentum, long-lived particle decays (e.g., $K^\pm$, K^0_L) and conversion electrons as the two main sources of background.

For the charged hadron cross section, approximately 17×10^6 MB events were analyzed. The luminosity was measured as $N_{\mathrm{BBC}}/\sigma_{\mathrm{BBC}}$ with $\sigma_{\mathrm{BBC}} = 21.8$ mb [21], accounting for the fraction of the yield for which the MB condition was satisfied. Backgrounds were estimated and subtracted statistically following the method of [22]: Conversion electrons were estimated using the different response of the ring-imaging Čerenkov detector (RICH) [23] to electrons and charged pions, and decay particles were estimated using the track bend in the residual magnetic field in the tracking detectors. Weak decays of short-lived particles, mainly K^0_S, Λ, and $\bar{\Lambda}$, remain, especially when they decay close to the vertex. Based on a Monte Carlo simulation, the reported cross section was reduced by 7% over the entire p_T range to correct for these decays.

The unpolarized cross section for inclusive charged hadron production at midrapidity is presented in Fig. 1 and Table I. The dominant systematic uncertainty for $p_T > 5$ GeV/c is from the background subtraction, while for $p_T < 5$ GeV/c it is due to the weak-decay correction.
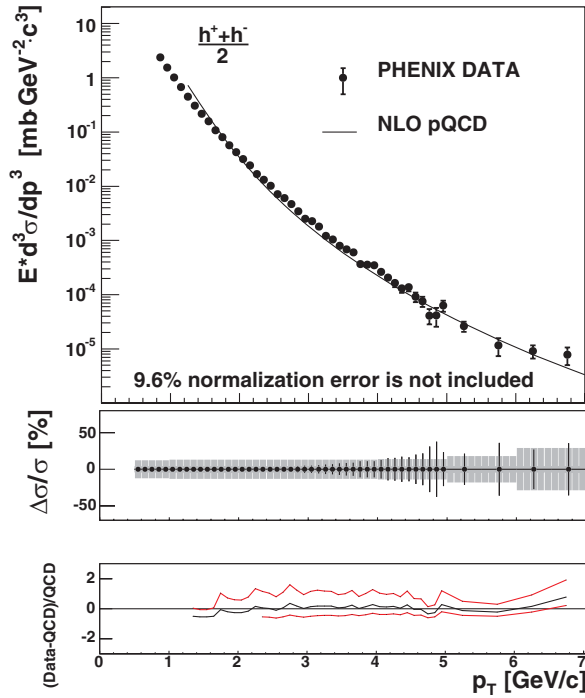
FIG. 1 (color online).   Top panel: Invariant cross section vs p_T for the production of charged hadrons at midrapidity, averaged over sign. A 9.6% normalization uncertainty is not shown. The curve represents a NLO pQCD calculation at a renormalization scale of p_T [26]. Middle panel: The relative statistical (points) and point-to-point systematic (band) errors. Bottom panel: The relative difference between the data and the theory with scales of $p_T/2$ (lower curve), p_T, and $2p_T$ (upper curve).

There is a 9.6% normalization uncertainty due to the luminosity measurement. In Fig. 1 the cross section is compared to a next-to-leading-order (NLO) perturbative QCD (pQCD) calculation using the CTEQ6M [24] parton distribution functions and Kniel-Kramer-Pötter FFs [25] and found to be consistent above $p_T \sim 2$ GeV/c. The unpolarized cross sections for midrapidity and forward production of neutral pions have also been measured in 200 GeV proton-proton collisions at RHIC [8,21] and have been found to agree well with NLO pQCD calculations [26–28]. This agreement between all of these unpolarized measurements and theory indicates that NLO pQCD is applicable in interpreting polarized data at $\sqrt{s} =$ 200 GeV and provides a solid theoretical foundation for the study of the spin structure of the proton at RHIC.

The stable spin direction of the protons through acceleration and storage is vertical, and there is an approximately equal number of bunches filled with the spin of the protons up as there is down. With both beams polarized, single-spin analyses were performed by taking into account the spin states of one beam, averaging over those of the other. The beam polarization at 100 GeV was obtained using the same analyzing power (A_N^{pC}) in proton-carbon elastic scattering in the Coulomb-nuclear interfer-

TABLE I.   Selected invariant cross section values for $(h^+ + h^-)/2$ corresponding to Fig. 1. A 9.6% normalization uncertainty is not included.

p_T (GeV/c)	Invariant cross section (mb/GeV^2)	Statistical error (%)	Systematic error (%)
0.55	1.06×10^1	0.2	8
1.05	1.02×10^0	0.4	8.5
1.55	1.58×10^{-1}	0.9	8.5
2.05	3.16×10^{-2}	1.7	9
2.55	7.14×10^{-3}	3.2	9
3.05	2.28×10^{-3}	5.1	9
3.55	6.86×10^{-4}	8.5	9
4.05	2.63×10^{-4}	12.8	9.5
4.55	9.12×10^{-5}	20.2	9.5
5.25	2.61×10^{-5}	21.2	16
5.75	1.16×10^{-5}	36.3	16
6.25	9.12×10^{-6}	27.2	28
6.75	7.82×10^{-6}	35.7	28

ence region measured at 22 GeV (see [29], and references therein), near RHIC injection energy. The average beam polarization was $15 \pm 5\%$.

The left-right transverse single-spin asymmetry, A_N, can be extracted using

$$A_N = \frac{1}{P_\mathrm{b}}\left(\frac{\sigma^\uparrow - \sigma^\downarrow}{\sigma^\uparrow + \sigma^\downarrow}\right) = \frac{1}{P_\mathrm{b}}\frac{1}{\langle|\cos\phi|\rangle}\left(\frac{N^\uparrow - \mathcal{R}N^\downarrow}{N^\uparrow + \mathcal{R}N^\downarrow}\right), \quad (1)$$

where P_b is the beam polarization, $\sigma^\uparrow$ ($\sigma^\downarrow$) the production cross section when the protons in the bunch are polarized up (down), $N^\uparrow$ ($N^\downarrow$) the experimental yield from up- (down-) polarized bunches, and $\mathcal{R} = \mathcal{L}^\uparrow/\mathcal{L}^\downarrow$ the relative integrated luminosity of bunches of opposite polarization sign. The azimuthal term accounts for the coverage of the central arms. The above formula as written applies to yields observed to the left of the polarized beam. An overall minus sign is required for yields observed to the right of the polarized beam. Alternatively, we derive the asymmetry using

$$A_N = \frac{1}{P_\mathrm{b}}\frac{1}{\langle|\cos\phi|\rangle}\left(\frac{\sqrt{N_L^\uparrow N_R^\downarrow} - \sqrt{N_L^\downarrow N_R^\uparrow}}{\sqrt{N_L^\uparrow N_R^\downarrow} + \sqrt{N_L^\downarrow N_R^\uparrow}}\right), \quad (2)$$

which calculates a single value for the asymmetry taking into account yields from both the left (N_L) and right (N_R) sides of the polarized beam and provides a consistency check on the relative luminosity [30].

The BBCs were used to determine the relative luminosity [$\mathcal{R}$ in Eq. (1)] between bunches of opposite polarization sign fill-by-fill. A typical $\mathcal{R}$ for the data sample analyzed here was approximately 1.09, measured to better than 10^{-3}. In the asymmetry analysis of charged hadrons, which utilized ~ 13 M minimum-bias events, it was required that

TABLE II. Neutral pion transverse single-spin asymmetry values and statistical uncertainties for all photon pairs falling within the π^0 mass peak, for the background (bg), and for the π^0 background corrected. The third column (r) indicates the background contribution under the π^0 peak. An A_N scale uncertainty of $\pm 35\%$ is not included.

p_T (GeV/c)	$\langle p_T \rangle$ (GeV/c)	r (%)	A_N^{peak} (%)	A_N^{bg} (%)	$A_N^{\pi^0}$ (%)
1–2	1.45	34	-0.6 ± 0.8	-0.7 ± 0.9	-0.5 ± 1.2
2–3	2.34	12	-1.4 ± 1.7	-3.1 ± 3.4	-1.2 ± 2.0
3–4	3.36	6	-1.3 ± 4.2	3.6 ± 12.2	-1.6 ± 4.7
4–5	4.38	5	7.0 ± 10.1	42 ± 39	5.2 ± 10.9

there be no hits in the RICH in order to eliminate electrons from photon conversions which mimic high-p_T charged tracks. The momentum threshold for production of Čerenkov radiation by pions was 4.7 GeV/c, allowing the RICH veto to preserve nearly all charged pions. The electron contamination in the final data sample was less than 1%. The decay background from long-lived particles was less than 5%.

Neutral pions were reconstructed via their decay to two photons using finely segmented ($\Delta\phi \times \Delta\eta \approx 0.01 \times 0.01$) electromagnetic calorimeters (EMCal) [31]. Photon clusters were selected by their shower shape and a charged track veto. Approximately 18 M events recorded by an EMCal–based high-energy photon trigger in coincidence with the BBC collision trigger were analyzed [21]. The trigger efficiency for neutral pions varied from ∼24% in the 1–2 GeV/c bin to ∼78% in the 4–5 GeV/c bin. Only triggered events were used in this analysis. The π^0 peak widths varied from 13.2 MeV/c^2 in the 1–2 GeV/c bin to 10.6 MeV/c^2 in the 4–5 GeV/c bin. The contribution from combinatorial background ranged from 34% to 5% across these bins; in order to avoid errors associated with peak extraction it was not subtracted.

The asymmetry for neutral pions and charged hadrons was determined for each fill using Eq. (1), then averaged over all fills. The contribution to the π^0 asymmetry by the background under the peak was estimated by calculating the asymmetry of 50 MeV/c^2 regions on both sides of the signal, from 60–110 MeV/c^2 and 170–220 MeV/c^2 (see Table II). The asymmetry of the signal region and its uncertainty were then corrected using

$$A_N^{\pi^0} = \frac{A_N^{\text{peak}} - rA_N^{\text{bg}}}{1-r}, \qquad \sigma_{A_N^{\pi^0}} = \frac{\sqrt{\sigma^2_{A_N^{\text{peak}}} + r^2\sigma^2_{A_N^{\text{bg}}}}}{1-r}, \quad (3)$$

where r is the fraction of background under the peak.

As the dominant systematic uncertainty is expected to be from the determination of the relative luminosity, systematic errors were evaluated by direct comparison of the asymmetry values calculated using Eqs. (1) and (2). Any potential effect should be the same for both the charged hadron and neutral pion analyses. No p_T dependence was expected or observed; therefore, we take the weighted average of the systematic uncertainties calculated for

each bin, 0.002, as the overall, uniform systematic uncertainty.

The asymmetries are plotted vs p_T in Fig. 2 and shown in Tables II and III. The asymmetries are consistent with zero over the entire transverse momentum range.

In this Letter we have presented the first measurement of transverse-spin asymmetries A_N at midrapidity and high p_T at collider energies and the cross section for inclusive charged hadrons at midrapidity. NLO pQCD calculations have been found to reproduce experimental results for $p_T \gtrsim 2$ GeV/c not only for the cross section presented here but also for inclusive neutral pion production, indicating that pQCD can be used to interpret the high-p_T asymmetries. The transverse SSAs observed for midrapidity production of both neutral pions and charged hadrons are consistent with zero within statistical errors of a few percent, measured over $0.5 < p_T < 5$ GeV/c. The result is consistent with the midrapidity results for neutral pions at $\sqrt{s} = 20$ GeV [9]. The present measurement is complementary to that of [8]. The large asymmetries observed in neutral pion production at forward rapidity at $\sqrt{s} = 200$ GeV [8] are expected to originate from partonic processes involving valence quarks ($x > 0.1$), whereas the
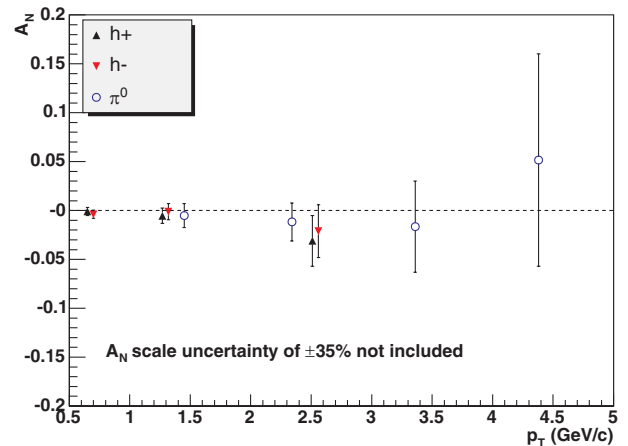

FIG. 2 (color online). Midrapidity neutral pion and charged hadron transverse single-spin asymmetry A_N vs transverse momentum. Points for positive hadrons have been shifted down by 50 MeV/c to improve readability. The error bars indicate statistical uncertainties.

TABLE III. Charged hadron transverse single-spin asymmetry values and statistical uncertainties. An A_N scale uncertainty of $\pm 35\%$ is not included.

p_T (GeV/c)	$\langle p_T \rangle$ (GeV/c)	$A_N^{h^-}$ (%)	$A_N^{h^+}$ (%)
0.5–1	0.70	-0.38 ± 0.42	-0.09 ± 0.41
1–2	1.32	-0.12 ± 0.82	-0.54 ± 0.78
2–5	2.56	-2.1 ± 2.7	-3.1 ± 2.6

particle production at midrapidity presented here is dominated by gluon-gluon and quark-gluon processes ($x < 0.1$). Our results are consistent with the pQCD expectation that quark-gluon correlations are suppressed at high p_T and midrapidity [15,32]. A QCD analysis of the presented A_N may lead to constraints on gluon-Sivers contributions to observed transverse-spin phenomena. The present transverse single-spin asymmetries represent an early measurement in a rigorous program to study transverse proton spin structure at hard scales using a pQCD framework at RHIC.

———

*Deceased.
†PHENIX Spokesperson.
Electronic address: zajc@nevis.columbia.edu

[1] W. H. Dragoset *et al.*, Phys. Rev. D **18**, 3939 (1978).
[2] C. E. Allgower *et al.*, Phys. Rev. D **65**, 092008 (2002).
[3] J. Antille *et al.*, Phys. Lett. B **94**, 523 (1980).
[4] S. Saroff *et al.*, Phys. Rev. Lett. **64**, 995 (1990).
[5] V. D. Apokin *et al.*, Phys. Lett. B **243**, 461 (1990).
[6] D. L. Adams *et al.*, Phys. Lett. B **261**, 201 (1991).
[7] D. L. Adams *et al.*, Phys. Lett. B **264**, 462 (1991).
[8] J. Adams *et al.*, Phys. Rev. Lett. **92**, 171801 (2004).
[9] D. L. Adams *et al.*, Phys. Rev. D **53**, 4747 (1996).
[10] A. Airapetian *et al.*, Phys. Rev. Lett. **84**, 4047 (2000).
[11] A. Airapetian *et al.*, Phys. Lett. B **535**, 85 (2002).
[12] A. Airapetian *et al.*, Phys. Rev. Lett. **94**, 012002 (2005).
[13] J. C. Collins, Nucl. Phys. **B396**, 161 (1993).
[14] D. Sivers, Phys. Rev. D **41**, 83 (1990).
[15] J. Qiu and G. Sterman, Phys. Rev. D **59**, 014004 (1999).
[16] Y. Kanazawa and Y. Koike, Phys. Lett. B **478**, 121 (2000).
[17] M. Burkardt and D. S. Hwang, Phys. Rev. D **69**, 074032 (2004).
[18] K. Adcox *et al.*, Nucl. Instrum. Methods Phys. Res., Sect. A **499**, 469 (2003).
[19] M. Allen *et al.*, Nucl. Instrum. Methods Phys. Res., Sect. A **499**, 549 (2003).
[20] K. Adcox *et al.*, Nucl. Instrum. Methods Phys. Res., Sect. A **499**, 489 (2003).
[21] S. S. Adler *et al.*, Phys. Rev. Lett. **91**, 241803 (2003).
[22] S. S. Adler *et al.*, Phys. Rev. C **69**, 034910 (2004).
[23] M. Aizawa *et al.*, Nucl. Instrum. Methods Phys. Res., Sect. A **499**, 508 (2003).
[24] J. Pumplin *et al.*, J. High Energy Phys. 07 (2002) 012.
[25] B. A. Kniehl, G. Kramer, and B. Pötter, Nucl. Phys. **B597**, 337 (2001).
[26] B. Jäger, A. Schäfer, M. Stratmann, and W. Vogelsang, Phys. Rev. D **67**, 054005 (2003).
[27] F. Aversa, P. Chiappetta, M. Greco, and J. P. Guillet, Nucl. Phys. **B327**, 105 (1989).
[28] D. de Florian, Phys. Rev. D **67**, 054004 (2003).
[29] O. Jinnouchi *et al.*, AIP Conf. Proc. **675**, 817 (2003).
[30] H. Spinka, Argonne National Laboratory Report No. ANL-HEP-TR-99-113, 1999.
[31] L. Aphecetche *et al.*, Nucl. Instrum. Methods Phys. Res., Sect. A **499**, 521 (2003).
[32] G. L. Kane, J. Pumplin, and W. Repko, Phys. Rev. Lett. **41**, 1689 (1978).